Physica Medica 65 (2019) 15–20

Contents lists available at ScienceDirect

Physica Medica

journal homepage: www.elsevier.com/locate/ejmp

Original paper

Evaluation of silica and PMMA optical fibre response when irradiated with 16.5 MeV protons

Johan Asp[a,b], Alexandre M. Caraça Santos[c,d,*], Shahraam Afshar V.[b,d], Wen Qi Zhang[b], Eva Bezak[d,e]

[a] South Australian Health and Medical Research Institute, Adelaide, Australia
[b] Division of Information Technology, Engineering and Environment, School of Engineering, The University of South Australia, Australia
[c] Department of Radiation Oncology, Royal Adelaide Hospital, Adelaide, Australia
[d] School of Physical Sciences and Institute for Photonics and Advanced Sensing, University of Adelaide, Australia
[e] Cancer Research Institute and the School of Health Sciences, University of South Australia, Adelaide, Australia

ARTICLE INFO

Keywords:
Fibre optic luminescence dosimetry
Radioluminescence
Protons

ABSTRACT

An investigation into the response of optical fibres to 16.5 MeV protons is presented here. A silica and a poly (methyl methacrylate) (PMMA) optical fibre was exposed to 16.5 MeV protons from a GE PETtrace cyclotron. The optical fibres were exposed to beam currents of 30nA – 270nA and the emission spectrum analysed. The silica fibre was the most sensitive and had two main peaks at 460 nm and 650 nm. The ratio between the peaks was observed to increase as irradiation of the fibres continued, where the 460 nm peak increased at a rate > 4 times the 650 nm peak. The rate of increase of the ratio between the peaks was observed to be constant at a constant target current and linear with target current. In the case of the PMMA fibre, significant spectral changes were observed during the exposure to 16.5 MeV protons. A simple method for estimating the effect of photodarkening and activation is presented here and indicated that the changes in the spectrum for the PMMA fibres may be due to photodarkening and activation.

1. Introduction

Recently, there have been numerous studies evaluating bare optical fibres used as radiation dosimeters in proton beams [1–4]. These dosimetry systems are real-time and can be made using quite thin optical fibres, resulting in a high spatial resolution. One major advantage being reported is that the light output from the bare optical fibres may exhibit minimal ionisation quenching free, and therefore be suitable for measurement of the absorbed dose in the Bragg peak [1].

Plastic optical fibres have been shown to have a linear dose response, high spatial resolution and exhibit minimal quenching effect for proton dosimetry [5,6]. There is, however, uncertainty in the published literature regarding the origin of the light emission in the plastic optical fibres. Jang et al. firstly reported that light was entirely Cerenkov radiation [6], Darafsheh et al. showed that the spectrum measured was not Cerenkov radiation [7,8], more recently Christensen et al. reported that the light generated is both fluorescence and Cerenkov [3].

Silica optical fibres have also been shown to have similar properties as the plastic optical fibres. Their emission has been observed to have two main peaks at 460 nm and 650 nm [1]. Darafsheh et al. reported that while the 650 nm peak had a linear dose dependence and quenching free response, the 460 nm peak did not and that the ratio of the peaks varied with proton penetration depth in a material at the Bragg peak for 100 MeV proton [1,9,10]. They concluded that the change in the peak ratios was possibly a linear energy transfer dependence.

The source of the 460 nm peak are oxygen deficiency centres, while the 650 nm peak is associated with non-bridging oxygen hole centres. Zhurenko et al. reported the peak ratio in silica optical fibres to change with accumulated dose for irradiation using protons of 210 keV [11,12]. They have shown that during irradiation the protons passivated the non-bridging oxygen hole centres and modified the oxygen deficiency centres, affecting the shape of the luminescence spectrum [12].

These studies discussed have shown both plastic and silica optical fibres to be potentially useful real-time dosimetry systems, including the development of array detectors [2,13,14]. Recently, there has been promising reports on the use of Ce3+ and Sb3+ doped fibres, which have a higher scintillation efficiency, for monitoring 18 MeV proton beams [15,16].

* Corresponding author at: Department of Radiation Oncology, Royal Adelaide Hospital, Adelaide, Australia.
E-mail address: alexandre.santos@adelaide.edu.au (A.M. Caraça Santos).

https://doi.org/10.1016/j.ejmp.2019.08.001
Received 23 March 2019; Received in revised form 19 July 2019; Accepted 1 August 2019
Available online 05 August 2019

In this study, the light output from a commercial silica and a poly (methyl methacrylate) (PMMA) optical fibre when exposed to 16.5 MeV protons is evaluated for their potential use as proton beam monitoring detectors for a radiobiological beam line of 16.5 MeV protons. Spectral changes were observed for both the silica and PMMA optical fibres as they accumulated dose. The dose response in the ratio between the 460 nm and 650 nm peaks was investigated for the silica optical fibre response. In the case of the PMMA optical fibres, a model was developed to predict the expected spectral changes due to photodarkening and activation of the PMMA. Photodarkening, or radiation induced colouration, is where the optical attenuation of the PMMA is changed due to its exposure to ionising radiation [17].

2. Experimental design

A 400 μm core diameter silica optical fibre (FVP400440480, Polymicro technologies, Molex, U.S.A.) and a 500 μm core diameter PMMA optical fibre (SH2001, Mitsubishi Rayon Co. LTD., Tokyo, Japan) were placed in the path of a 1 cm diameter, 16.5 MeV proton beam (GE PETtrace proton cyclotron, General Electric (GE) Healthcare, Uppsala, Sweden). The optical fibres were held on an aluminium plate, 20 cm away from the external beam port and were exposed to currents ranging from 25nA to 270nA, shown in Fig. 1. The optical fibres were 20 m long in order to guide the light generated by the optical fibres to the control room. Spectral analysis was performed using a spectrometer (QE65000, Ocean Optics Inc, U.S.A.).

The dose dependence of the fibre responses was evaluated by taking between 15 and 30 consecutive measurements. Each measurement was performed with a 20 s sampling period. The dose-rate dependence was evaluated by varying the beam current of the cyclotron. The dose that the fibres are being exposed to is given by:

$$D = A_{fibre}\frac{dx}{dm}\left[\rho\frac{dE}{dx}\right][\Phi dt] \quad (1)$$

where A_{fibre} is the area of the fibre (mm^2), dx is the diameter of the fibres (cm), dm is the mass of the fibre (kg), dE/dx is the proton electronic mass stopping power (J cm^2/g), dt is the irradiation time (s) and ρ is the medium density (g/cm^3). Φ is the proton flux ($mm^{-2}s^{-1}$) given by:

$$\Phi = \frac{I}{q}\left[\frac{1}{A_{beam}}\right] \quad (2)$$

where I is the beam current (A), q is the charge of the proton (C) and A_{beam} is the area of the proton beam (mm^2). Using the values shown in Table 1 an approximate dose of 37.8 Gy/nAs and 31.3 Gy/nAs for the PMMA and silica optical fibres, respectively is computed.

Table 1
Values of the experimental setup for dose estimation. Proton stopping powers were obtained from NIST [18].

dx [cm]	0.05
q [C]	1.602×10^{-19}
A_{fibre} [mm^2]	5
A_{beam} [mm^2]	78.5
ρ_{silica} [g/cm^3]	2.65
ρ_{PMMA} [g/cm^3]	1.18
dm_{silica} [kg]	6.63×10^{-6}
dm_{PMMA} [kg]	2.95×10^{-6}
dE/dx_{silica} [J cm^2/g]	4.76×10^{-12}
dE/dx_{PMMA} [J cm^2/g]	3.93×10^{-12}

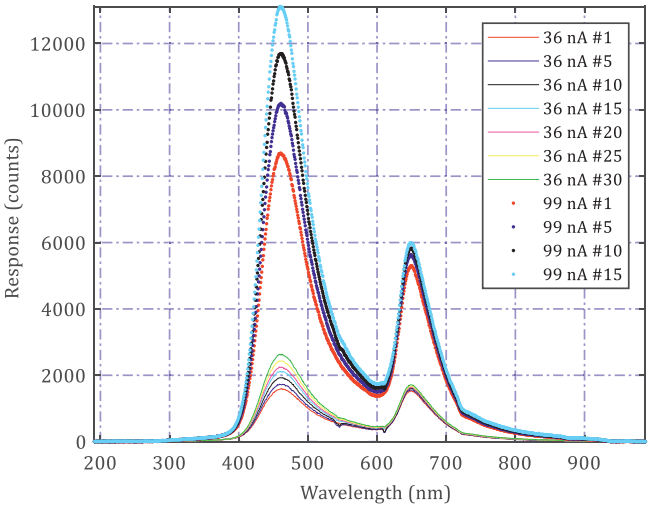

Fig. 2. The spectral response of the silica optical fibre consecutive exposures at 36 nA and 99 nA target currents.

3. Silica optical fibres

3.1. Spectral analysis

The measured spectrum from the silica optical fibres for a subset of the consecutive exposures is shown in Fig. 2. Two main peaks were observed at 460 nm and 650 nm. The increase in dose-rate via increasing the target current, results in an increase in the intensity of the response of the silica optical fibre. However, the intensity is also observed to increase after each of the consecutive exposures. Hence indicating an accumulated dose dependence or an activation of the fibre

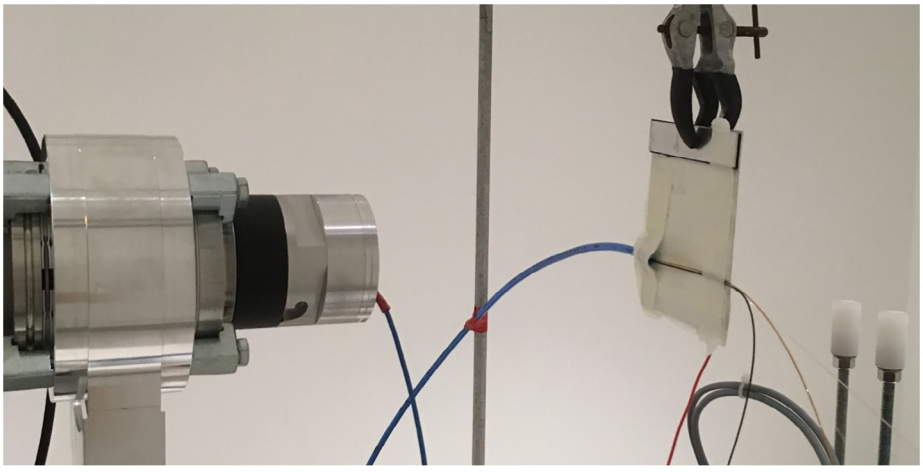

Fig. 1. The experimental setup of the optical fibres placed 20 cm away from the beam port.

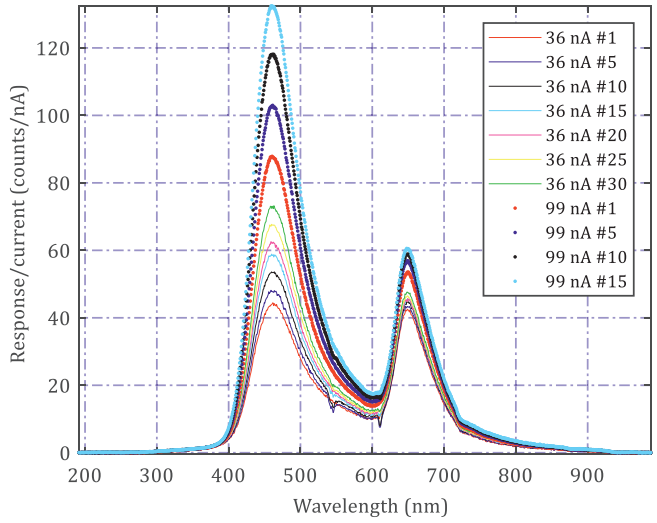

Fig. 3. The spectral response of the silica optical fibre divided by the target current, for consecutive exposures at 36 nA and 99 nA target currents.

and/or aluminium holder plate.

Fig. 3 shows the response of the silica optical fibres divided by the target currents. This further emphasises that the response of the optical fibres are not constant for a constant dose-rate, and is in fact continually increasing in intensity.

The 460 nm peak was integrated between 390 nm and 545 nm, the 650 nm was integrated between 600 nm and 735 nm. Fig. 4a) shows the mean integrated counts for both of the peaks. As can be observed they both continuously increase as the exposure continues. However, they are increasing at different rates. Fig. 4b) shows the change in response of each of the peaks during the exposure. It can be observed that the 460 nm peak is increasing at a faster rate than the 650 nm peak. The 460 nm peak is also observed to be increasing faster compared to the 650 nm peak for the 99nA than then 36nA, 5.4 times and 4.4 times faster, respectively. However, the change in the mean peak counts is not constant for the constant dose rate exposure.

4. Peak ratios

Due to the differing change in intensity between the peaks, this was further investigated by evaluating the ratio between the peaks. Fig. 5 shows the change in the ratio between the peaks during exposure. The change in the ratio between the two peaks at 650 and 460 nm is observed to be more constant than that observed for the individual peaks.

The change in response of the 460 nm peak, the 650 nm peak, the total counts across the measured spectrum and the ratio between the two peaks were measured to be 7.72 ± 1.25, 6.20 ± 2.76, 7.41 ± 1.47 and 2.17 ± 0.26, respectively. The 650 nm peak is observed to be the least reproducible of all, while the 460 nm peak and total counts result in quite similar results. While the ratio between the peaks is the least sensitive, it is by far the most reproducible and linear. Considering the current was increased by 2.75 times, the ratio between the peaks increased by 2.17.

The changing ratio between the two peaks for silica optical fibres has been previously reported for proton dosimetry [10]. It had been concluded that this may be a linear energy transfer dependence. In this study, the ratio was observed to change under constant irradiation and LET conditions. This could be a result of an accumulated dose dependence on the optical fibre. Further work is required to investigate the origin of the differing peaks.

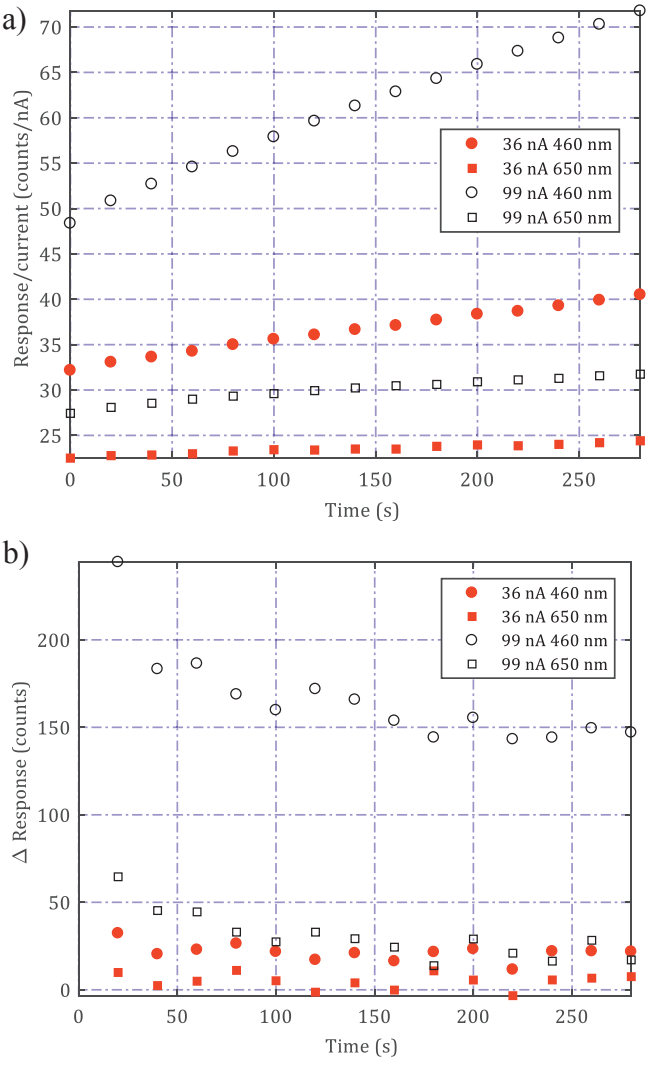

Fig. 4. a) The mean counts divided by the beam current, of the two peaks during exposure, and b) the change in the mean counts.

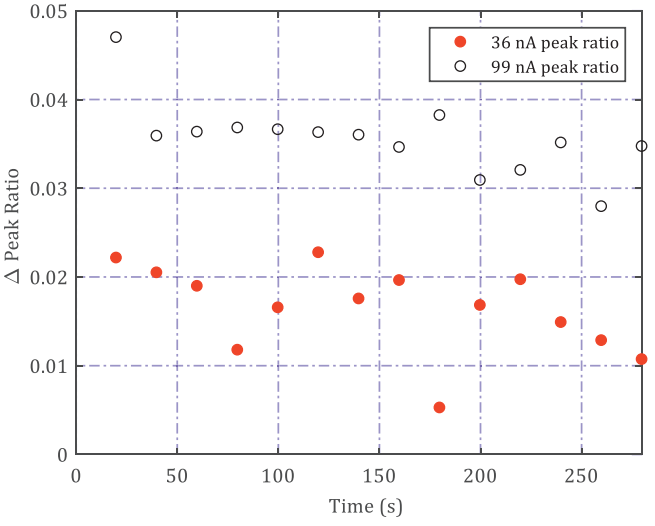

Fig. 5. The change in the ratio between the 460 nm and 650 nm peaks.

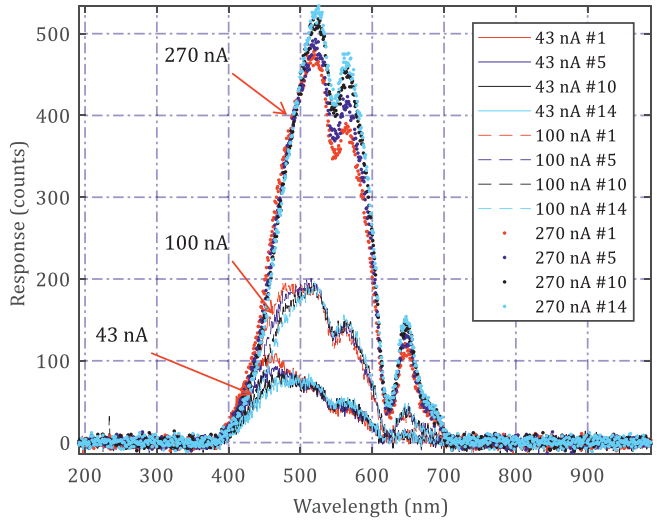

Fig. 6. The spectral response of the PMMA optical fibre consecutive exposures at 43 nA, 100 nA and 270 nA target currents.

5. PMMA optical fibres

5.1. Spectral analysis

The measured spectrum from the PMMA optical fibre for a subset of the consecutive exposures is shown in Fig. 6. The increase in dose-rate via increasing the target currents results in an increase in the intensity of the response of the PMMA optical fibre. Fig. 6 show three distinct groups of spectral data for the three currents. However, the spectrum is also observed to significantly alter after each of the consecutive exposures.

Fig. 7 shows the PMMA measured spectrums divided by their target currents. It can be observed the major changes in the emission from the optical fibre as exposure continues. It was observed that the emission from the lower wavelengths was reducing while the intensity from the higher wavelengths increased.

Fig. 8a) shows the total integrated counts for each of the measurements divided by their target current. Surprisingly, while there are variations in the optical spectrum from the PMMA the total integral light stays somewhat constant. Fig. 8b) shows the mean of the integrals counts with a linear fit, where the error bars represent one standard deviation from the mean. It can be observed that the response of the integrated counts from the PMMA optical fibre is linear with dose rate.

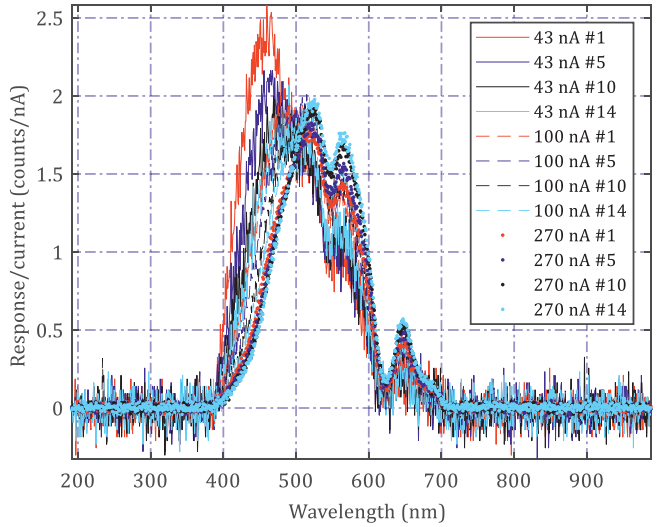

Fig. 7. The spectral response of the PMMA optical fibre divided by the target current, for consecutive exposures at 43 nA, 100 nA and 270 nA target currents.

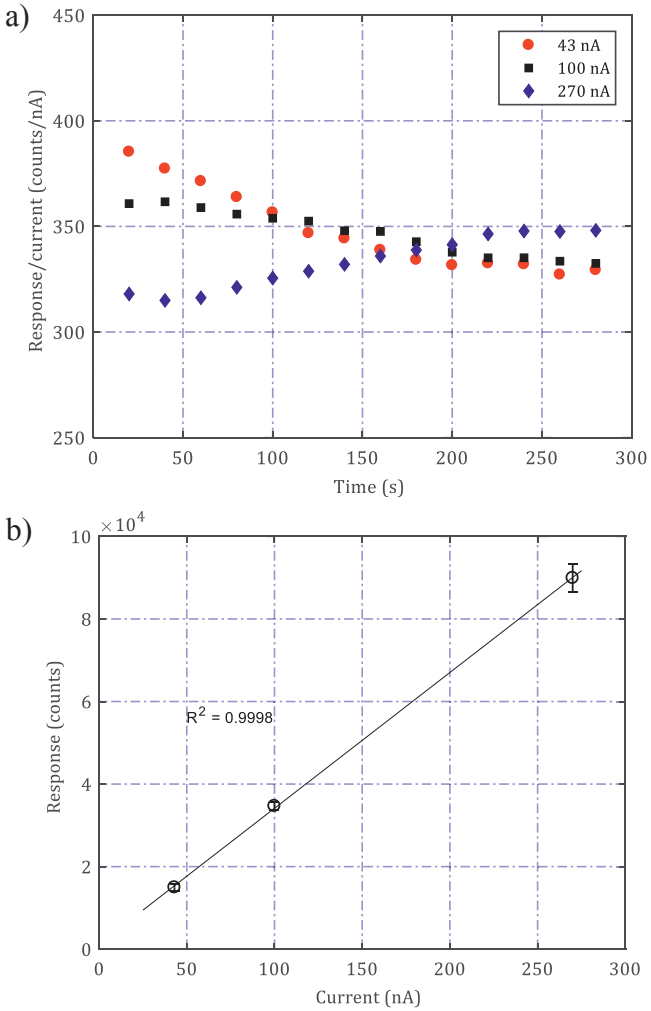

Fig. 8. a) The integrated total counts for the PMMA optical fibre and b) the mean of the integrated total counts with a linear fit, where the error bars represent the standard deviation.

6. Activation and photodarkening correction

The optical spectral changes observed for the PMMA optical fibre being continuously exposed by a proton beam was hypothesised to be due to two components. Firstly, that the 16.5 MeV protons are activating the optical fibre itself and the neighbouring area such that there is an increasing dose-rate to the optical fibre as exposure continues. Hence, the dose-rate, $\dot{D}$, exposed to the optical fibre is given by Eq. (3):

$$\dot{D}(t) \propto A + R \times t \times A. \tag{3}$$

where t is the time, A is the target current and R is an activation coefficient. R can be interpreted as a combination of the activation build up and radioactive decay during the exposure. Therefore the expected spectrum, $f(\lambda,t)$, is defined as:

$$f(\lambda, t) = \frac{f(\lambda, t = 0)}{\dot{D}(t = 0)} \times \dot{D}(t). \tag{4}$$

The second component is that there is some photodarkening occurring within the core of the PMMA optical fibre. This may result in a differing non-linear optical attenuation within the core which is altering the optical spectrum observed. To model this, we consider the optical attenuation coefficient, $\alpha(\lambda, t)$, that is related to the input

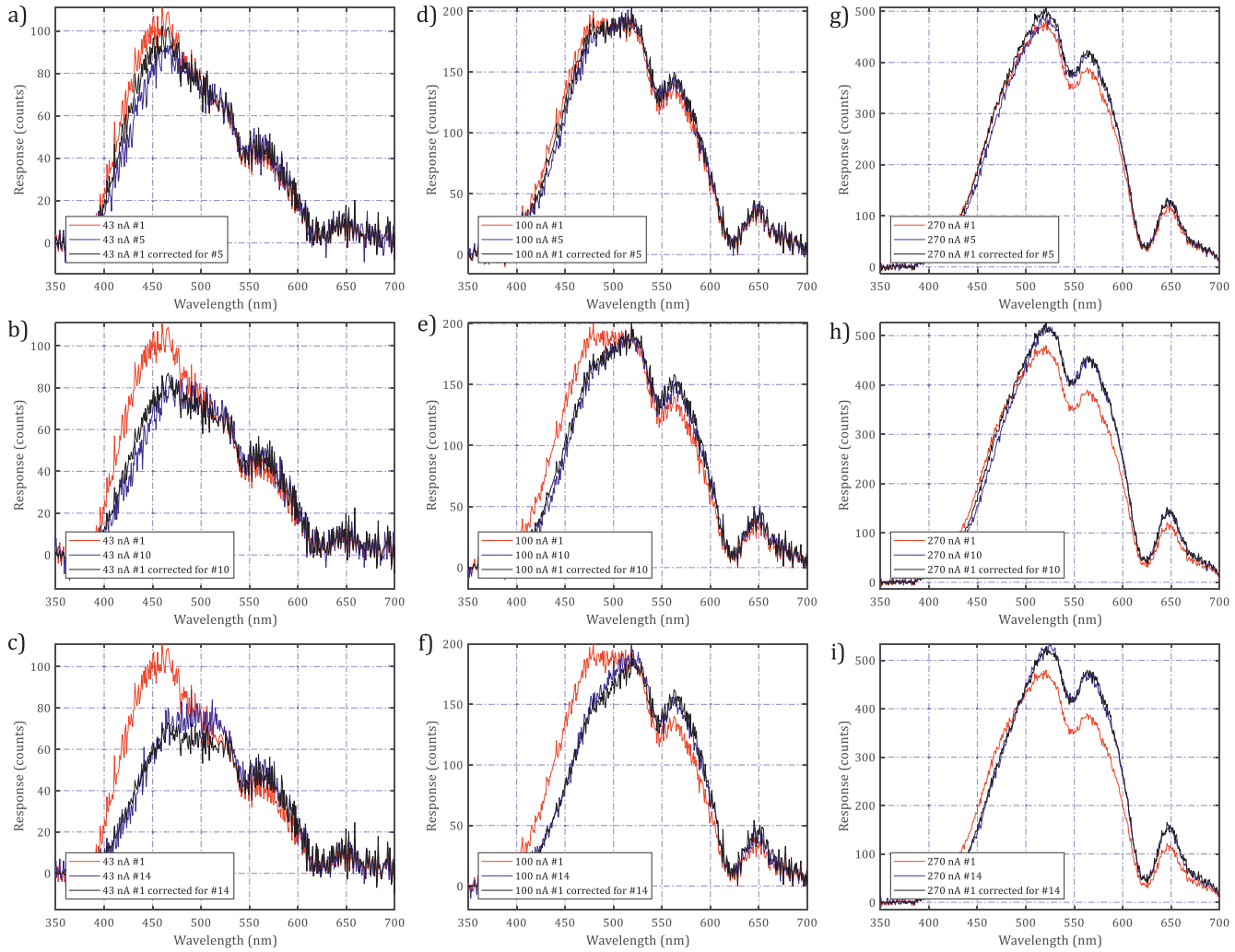

Fig. 9. The modelled spectrum accounting for photo-darkening and activation of the PMMA optical fibre after the first measurement for 43 nA; at the a) 5th (t = 100 s), b) 10th (t = 200 s) and c) 14th (t = 280 s), 100 nA; at the d) 5th (t = 100 s), e) 10th (t = 200 s) and f) 14th (t = 280 s), and for 270 nA; at the g) 5th (t = 100 s), h) 10th (t = 200 s) and i) 14th (t = 280 s).

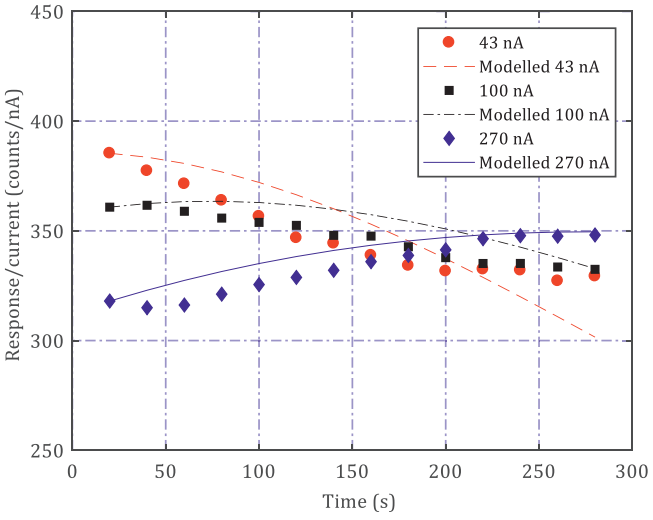

Fig. 10. The measured and modelled total counts accounting for photo-darkening and activation of the PMMA optical fibre after the first measurement for 43 nA, 100 nA and 270 nA exposures.

spectrum, and the output spectrum, $f'(\lambda,t)$, by Eq. (5):

$$\alpha(\lambda, t) = 10 \times \log_{10}\left(\frac{f(\lambda, t)}{f'(\lambda, t)}\right). \tag{5}$$

Using this we define the dose-rate dependent attenuation coefficient, as:

$$\alpha(\lambda, t) = C \times \alpha_{photo}(\lambda) \times \dot{D}(t) \times t, \tag{6}$$

where $\alpha_{photo}(\lambda)$ is the measured optical attenuation at wavelength λ, and C is a constant. Hence the optical spectrum can now be modelled from the first measured spectrum at t = 0. To estimate the effects of activation and photodarkening, one can rearrange Eq. (5) for the output spectrum, $f'(\lambda,t)$, and substitute the $\alpha(\lambda, t)$ defined in Eq. (6) to obtain Eq. (7):

$$f'(\lambda, t) = \frac{f(\lambda, t=0)}{\dot{D}(t=0)} \times \left[\frac{(A + R \times t \times A)}{10^{\frac{C \times t \times \alpha_{photo}(\lambda) \times (A + R \times t \times A)}{10}}}\right]. \tag{7}$$

Optical attenuation data for PMMA, $\alpha_{photo}(\lambda)$, was obtained from Fernandez et al. [17]. Fig. 9 show a subset of the modelled spectral changes from the first measured compared to the actual measure after that given time. R values of 0.03 s^{-1}, and C values of 0.00025 nC, 0.0001 nC and 0.000025 nC, were used for the 43 nA, 100 nA and 270 nA, respectively. These values were obtained iteratively, and a

Table 2
PACE4 simulation results for isotopes produced from the aluminium plate, silica and PMMA.

Material	Elemental composition	Produced isotopes	Yield %	Half life
Aluminium	^{27}Al	^{27}Si	10.2	4.2 s
Silica (SiO_2)	^{28}Si	^{25}Al	1.3	7.2 s
	^{16}O	^{13}N	24.7	10 m
		^{17}F	0.4	64.4 s
PMMA ($C_5O_2H_8$)n	^{12}C	^{13}N	0.02	10 m
	^{16}O	^{13}N	24.7	10 m
		^{17}F	0.4	64.4 s

good visual agreement was found between measured and modelled spectral distribution. Fig. 10 shows the total integral counts of the modelled data alongside the measured total counts. The modelled data is generally in good agreement with the measured. Hence, the changes observed for the PMMA optical fibre do indicate to be from photodarkening and activation.

7. Discussion

To evaluate the possibility of additional signal due to activation products produced in the experiment, the possible produced isotopes were simulated using Projection Angular-momentum coupled Evaporation (PACE4) software [19,20]. Table 2 shows the results of the PACE4 simulations for the aluminium plate, silica and PMMA optical fibres when exposed to protons of 16.5 MeV. There are a number of short-lived radioisotopes produced in either the plate holder or optical fibres which could contribute to the increase in the signal observed by the optical fibres during the constant exposure.

8. Conclusion

The response of a commercial silica and PMMA optical fibre to 16.5 MeV protons was investigated. Both optical fibres were found to have a varying response under a constant beam current exposure.

The emission from the PMMA optical fibres was observed to significantly change during the irradiation. While the relative spectral changes were quite obvious, the total integral counts did not change substantially and the response was observed to be linear with target current. The increase in dose-rate due to activation of the region along with the photodarkening of the PMMA was modelled. The results indicate that the spectral changes observed could be due to photodarkening and activation.

Two emission peaks were observed for the silica optical fibre, at 460 nm and 650 nm. It was observed that during exposure that both peaks intensity continued to rise but at different rates. The ratio between the two peaks was evaluated and found that the rate of increase in the ratio was constant for a constant target current. The rate of increase in the ratio between the peaks was also observed to increase linearly with the target current. This increase in emission may also be due to activation occurring when exposed to the protons similar to that shown for the PMMA.

References

[1] Darafsheh A, Zhang R, Kassaee A, Finlay JC. Characterization of the proton irradiation induced luminescence of materials and application in radiation oncology dosimetry. SPIE BiOS: SPIE; 2018. p. 7.
[2] Son J, Lee S, Lim Y, Park S, Cho K, Yoon M, et al. Development of optical fiber based measurement system for the verification of entrance dose map in pencil beam scanning proton beam. Sensors 2018;18:227.
[3] Jeppe Brage C, Erik A, Håkan N, Claus EA. Quenching-free fluorescence signal from plastic-fibres in proton dosimetry: understanding the influence of Čerenkov radiation. Phys Med Biol 2018;63:065001.
[4] Hwang U-J, Shin D, Lee SB, Lim YK, Jeong JH, Kim HS, et al. Depth dose measurement using a scintillating fiber optic dosimeter for proton therapy beam of the passive-scattering mode having range modulator wheel. J Korean Phys Soc 2018;72:1025–32.
[5] Son J, Kim M, Jeong J, Lim Y, Lee SB, Shin D, et al. Characteristics of fiber-optic radiation sensor for passive scattering proton beams. J Instrum 2017;12:P11015.
[6] Jang KW, Yoo WJ, Shin SH, Shin D, Lee B. Fiber-optic Cerenkov radiation sensor for proton therapy dosimetry. Opt Express 2012;20:13907–14.
[7] Darafsheh A, Taleei R, Kassaee A, Finlay JC. The visible signal responsible for proton therapy dosimetry using bare optical fibers is not Čerenkov radiation. Med Phys 2016;43:5973–80.
[8] Darafsheh A, Taleei R, Kassaee A, Finlay JC. On the origin of the visible light responsible for proton dose measurement using plastic optical fibers. SPIE BiOS 2017;10056:5.
[9] Darafsheh A, Taleei R, Kassaee A, Finlay JC. Proton therapy dosimetry using the scintillation of the silica fibers. Opt Lett 2017;42:847–50.
[10] Darafsheh A, Taleei R, Kassaee A, Finlay JC. Proton therapy dosimetry by using silica glass optical fiber microprobes. SPIE BiOS 2017;10058:4.
[11] Zhurenko VP, Kalantaryan OV, Kononenko SI. Change of silica luminescence due to fast hydrogen ion bombardment; 2015, 60:289.
[12] Kalantaryan O, Zhurenko V, Kononenko S, Barannik E, Kononenko O. Time dependence of silica optical properties during the implantation of fast hydrogen ions: Experiment. Nucl Instrum Methods Phys Res Sect B 2016;366:90–5.
[13] Son J, Kim M, Shin D, Hwang U, Lee S, Lim Y, et al. Development of a novel proton dosimetry system using an array of fiber-optic Cerenkov radiation sensors. Radiother Oncol 2015;117:501–4.
[14] Lo Presti D, Bonanno DL, Longhitano F, Bongiovanni DG, Russo GV, Leonora E, et al. Design and characterisation of a real time proton and carbon ion radiography system based on scintillating optical fibres. Phys Med Eur J Med Phys 2016;32:1124–34.
[15] Nesteruk KP, Auger M, Braccini S, Carzaniga TS, Ereditato A, Scampoli P. A system for online beam emittance measurements and proton beam characterization. J Instrum 2018;13:P01011.
[16] Auger M, Braccini S, Carzaniga TS, Ereditato A, Nesteruk KP, Scampoli P. A detector based on silica fibers for ion beam monitoring in a wide current range. J Instrum 2016;11:P03027.
[17] Fernandez AF, O'Keeffe S, Fitzpatrick C, Brichard B, Berghmans F, Lewis E. Gamma dosimetry using commercial PMMA optical fibres for nuclear environments. In 17th International Conference on Optical Fibre Sensors; 2005; 5855:4.
[18] Berger MJ, Coursey, J.S., Zucker, M.A., Chang, J. ESTAR, PSTAR, and ASTAR: Computer programs for calculating stopping-power and range tables for electrons, protons, and helium ions (version 2.0.1); 2005.
[19] Gavron A. Statistical model calculations in heavy ion reactions. Phys Rev C 1980;21:230–6.
[20] Tarasov OB, Bazin D. LISE++: Radioactive beam production with in-flight separators. Nucl Instrum Methods Phys Res Sect B 2008;266:4657–64.